2024 IEEE 63rd Conference on Decision and Control (CDC)
December 16-19, 2024. MiCo, Milan, Italy

On a Susceptible-Infected-Susceptible Epidemic Model with Reactive Behavioral Response on Higher-Order Temporal Networks

Lorenzo Zino and Alessando Rizzo

***Abstract*— We characterize the spread of epidemic diseases on higher-order temporal networks to shed light on the impact of large gatherings, where *superspreading events* occur and pairwise interactions are not sufficient to model the dynamics of infection. We propose a novel analytically-tractable continuous-time formalism for higher-order temporal networks based on the paradigm of activity-driven networks and we study a susceptible–infected–susceptible model spreading on top of it. By using a mean-field approach, we compute the epidemic threshold, characterizing a phase transition between a regime where the system converges to a disease-free equilibrium and one in which all trajectories converge to an endemic equilibrium. Using such a threshold, we quantify the role of higher-order interactions in favoring the spread of epidemic diseases, providing analytical support to restricting large gatherings during an epidemic outbreak. Finally, we incorporate a reactive behavioral response in the network formation process.**

I. Introduction

Epidemic modeling has become an important branch of research in the systems and control community [1]–[4]. The COVID-19 health crisis has brought further attention on this research direction, demonstrating how systems-theoretic approaches can offer useful tools to predict the evolution of an outbreak and inform interventions [5]–[9]. In particular, many diseases are transmitted through continuously-evolving pattern of contacts between individuals. Epidemic models on temporal networks have proved to be effective in capturing such transmission mechanism [4], [10]. One of the key drivers of epidemic diseases are large gatherings, which may become *superspreading events* [11]. Hence, during 2020–21, many public authorities banned such events, enforcing limitations on the maximum group size allowed to meet. Classical epidemic models on temporal networks, which are based on dynamical pairwise interactions between individuals, cannot capture and reproduce these group interactions, calling for the development of new mathematical approaches.

Higher-order networks have emerged as a powerful paradigm to study social interactions involving more than two individuals [12], [13]. Such paradigm, which has become increasingly popular in the physics community [14], [15], is still scarcely adopted in the systems and control community due to its limited analytical tractability. In fact, while the spread of epidemic diseases has been studied analytically on static higher-order networks [16], [17], the research on temporal higher-order networks mostly rely on Monte Carlo numerical simulations [15], [18]–[20]. Here, we aim at filling this gap by proposing a novel analytically-tractable framework for dynamics on higher-order temporal networks.

We propose a continuous-time model to describe higher-order temporal networks based on the paradigm of activity-driven networks (ADNs) [21], [22], motivated by the ability of ADNs to reproduce real-world interaction patterns [21] and their amenability to analytical treatment [23]–[25]. Then, we study a susceptible–infected–susceptible (SIS) model spreading on top of this temporal higher-order network. After deriving the exact dynamics of the Markov process that governs the epidemic spreading, we leverage a mean-field relaxation to obtain an analytically-tractable system of coupled nonlinear ordinary differential equations (ODEs) that approximate the emergent behavior of the epidemics [26]. Through the analysis of the asymptotic behavior of such system, we characterize a phase transition between two regimes: either the disease-free equilibrium (DFE) is globally asymptotically stable and the epidemic outbreak is quickly eradicated; or the DFE is unstable and trajectories converge to an endemic equilibrium (EE). Interestingly, we observe that the higher-order nature of social interactions seems to favor the spread of the epidemic disease, providing analytical support to the ban of large gatherings during an epidemic outbreak. Finally, we study the impact of human behavior, by incorporating a behavioral response in the model.

II. Model

Notation. We denote by $\mathbb{R}$, $\mathbb{R}_{\geq 0}$, $\mathbb{R}_{>0}$, and $\mathbb{Z}_{>0}$ the real, real nonnegative, strictly positive real, and strictly positive integer numbers, respectively. Given a function $x(t)$, we define $x(t^-) := \lim_{s \nearrow t} x(s)$ and $x(t^+) := \lim_{s \searrow t} x(s)$. A Poisson clock with rate $\rho \in \mathbb{R}_{>0}$ is a continuous-time stochastic process that clicks once in $[t, t+\Delta t]$ with probability equal to $\rho \Delta t + o(\Delta t)$, independent of the past, where $o(\Delta t)$ is the Landau little-O with respect to $\Delta t \searrow 0$.

A. Continuous-time higher-order activity-driven networks

We consider a population of $n \in \mathbb{Z}_{>0}$ individuals, $\mathcal{V} = \{1, \dots, n\}$. Each individual is identified by a node in an undirected higher-order temporal network $(\mathcal{V}, \mathcal{K}(t)), \in \mathbb{R}_{\geq 0}$, where $\mathcal{K}(t)$ is the set of simplicial complexes present in the network at time t. A simplicial complex is a graph-theoretic entity used to model interactions between two or multiple nodes, as illustrated in Fig. 1a. Specifically, a simplicial complex of order $m \in \mathbb{Z}_{>0}$ is a subset of $m+1$ distinct nodes $\kappa = \{v_1, v_2, \dots, v_{m+1}\} \subset \mathcal{V}$ that represents an interaction involving all the $m+1$ members of κ. In the simplest case

The authors are with the Department of Electronics and Telecommunications, Politecnico di Torino, Torino, Italy ({lorenzo.zino, alessandro.rizzo}@ polito.it). A. Rizzo is also with the Institute for Invention, Innovation, and Entrepreneurship, New York University Tandon School of Engineering, Brooklyn NY, US.

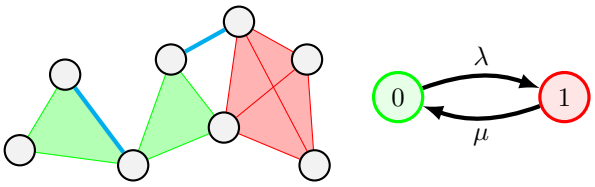

(a) Higher-order network (b) SIS model

Fig. 1: (a) Higher-order network with simplicial complexes of different order; (b) Transitions of an SIS model.

$m = 1$, a simplicial complex is just a pair of nodes, as a standard link in a network, representing pairwise interactions.

To generate the higher-order temporal network, inspired by [22], we define a continuous-time implementation of the simplicial activity-driven model proposed in [18], which we shall refer to as the continuous-time higher-order activity-driven network (hADN). Specifically, each individual is characterized by an activity rate $a_i \in \mathbb{R}_{>0}$, which captures the individual's tendency to initiate social interactions. Hence, such a higher-order network is generated as follows: i) at time $t = 0$, the we initialize $\mathcal{K}(t) = \emptyset$. Each node $i \in \mathcal{V}$ is associated with a Poisson clock with rate equal to a_i, each one independent of the others; ii) time progresses until any of the n Poisson clocks involved in the process clicks; iii) if the clock associated with node $i \in \mathcal{V}$ clicks at time t, individual i is *activated* and selects a m-uple of fellow individuals $j_1, \dots j_m$, selected uniformly at random among all possible m-uples of individuals; iv) the simplicial complex $\kappa = \{i, j_1, \dots, j_m\}$ is added to $\mathcal{K}(t)$; and v) the simplicial complex κ is immediately removed from the set, the Poisson process associated with node i is reinitialized, and the process is resumed from item ii).

B. Susceptible–infected–susceptible model

We consider an SIS epidemic process that spreads on the hADN. Each individual $i \in \mathcal{V}$ is associated with a state $x_i(t) \in \{0, 1\}$, $t \in \mathbb{R}_{\geq 0}$, and characterizes the individual's health state. Individuals can be either *susceptible* to the disease ($x_i(t) = 0$) or *infected* with the disease ($x_i(t) = 1$). States are gathered into the vector $\mathbf{x}(t) = [x_1(t) \dots x_n(t)]$, representing the state of the network at time t.

The state of each individual $i \in \mathcal{V}$, $x_i(t)$, evolves according to two contrasting mechanisms: contagion and recovery. If a susceptible individual i ($x_i(t^-) = 0$) has a contact with an infected individual at time t (i.e., if $\exists\, \kappa \in \mathcal{K}(t)$ such that $i, j \in \kappa$ and $x_j(t^-) = 1$), then i becomes infected ($x_i(t^+) = 1$) with probability $\lambda \in [0, 1]$, independent of the others. An infected individual ($x_i(t^-) = 1$) spontaneously recovers and becomes susceptible again ($x_i(t^+) = 0$) according to a Poisson clock with rate $\mu \in \mathbb{R}_{>0}$, independent of the others. A schematic of the SIS model is shown in Fig. 1b.

III. Dynamics

A. Markov process

Both the hADN formation process and the epidemic model are governed by independent Poisson processes. Hence, the state of the network $\mathbf{x}(t)$ evolves according to an n-dimensional continuous-time Markov process [27]. Accordingly, we can write the probability that a node $i \in \mathcal{V}$ switches its state in a time-interval of duration $\Delta t \in \mathbb{R}_{>0}$ as

$$\mathbb{P}[x_i(t + \Delta t) = b \,|\, x_i(t) = a] = q_i^{ab}(\mathbf{x}(t))\Delta t + o(\Delta t), \quad (1)$$

with $a, b \in \{0, 1\}$ and $b \neq a$. The coefficients $q_i^{01}(\cdot)$ and $q_i^{10}(\cdot)$ are the transition rates associated with the contagion and recovery of individual i, respectively, and their values, which may depend on time through the state of the system $\mathbf{x}(t)$, are computed in the following.

Proposition 1. *Consider an SIS model on a continuous-time hADN, the transition rates for a generic individual $i \in \mathcal{V}$ when $\mathbf{x}(t) = \mathbf{x}$ are equal to*

$$q_i^{01}(\mathbf{x}) = \lambda a_i \frac{m}{n-1} \sum_{j \in \mathcal{V}} x_j + \lambda \frac{m}{n-1} \sum_{j \in \mathcal{V}} a_j x_j + \lambda \frac{m(m-1)}{(n-1)(n-2)} \sum_{j \in \mathcal{V}} x_j \sum_{\ell \in \mathcal{V} \setminus \{i,j\}} a_\ell, \quad (2a)$$

$$q_i^{10}(\mathbf{x}) = \mu. \quad (2b)$$

Proof. The quantity $q_i^{01}(\mathbf{x})$ is the rate at which the susceptible individual i becomes infected, when $\mathbf{x}(t) = \mathbf{x}$. Individual i becomes infected if i has a contact with an infected individual and the disease is transmitted. We start by computing the rate at which i interacts with a generic individual j who is infected and the disease is transmitted, which we shall term $\alpha_{ij}(\mathbf{x})$. Then, since any infected individual $j \in \mathcal{V}$ can transmit the disease to i upon contact independently of the others, the total rate associated with contagion is simply obtained by summing all the rates [28], i.e., $q_i^{01}(\mathbf{x}) = \sum_{j \in \mathcal{V}} \alpha_{ij}(\mathbf{x})$.

To compute $\alpha_{ij}(\mathbf{x})$, we observe that i is infected by j if one of the following chains of events occurs: i) i activates, selects j among the m nodes selected in the simplicial complex, j is infected, and the disease is transmitted through the contact; ii) j is infected, j activates, selects i among the m nodes selected in the simplicial complex, and the disease is transmitted through the contact; iii) an individual $\ell \in \mathcal{V} \setminus \{i, j\}$ activates, ℓ selects both i and j among the m nodes selected in the simplicial complex, j is infected, and the disease is transmitted through the contact.

Using the properties of Poisson processes [28], we compute the rate at which each one of these chains of events occurs. For chain i) to occur, we need j to be infected. Then, the chain of events occurs according to the Poisson clock that regulates the activation of i, and by a sequence of two Bernoulli random variables, to account for the probability that j is selected and the probability that the disease is transmitted, respectively. Using the splitting property of Poisson processes [28], we compute its rate as the product between the activation rate a_i, the probability of selecting j when forming the simplicial complex (which is equal to $\frac{m}{n-1}$, since m individuals are sampled with no repetition) and the infection probability λ, yielding $\lambda a_i \frac{m}{n-1} x_j$, where the term x_j is an indicator function of the event "j is infected."

Similar, for ii), we multiply the activation rate of j (a_j) by the two probabilities $\frac{m}{n-1}$ and λ, and by the indicator function that j is infected, obtaining $\lambda a_j \frac{m}{n-1} x_j$.

Since the activation of each individual is independent of the others, iii) occurs with rate equal to the sum over all $\ell \in \mathcal{V} \setminus \{i,j\}$ of the product between the activation rate a_ℓ, the probability of selecting both i and j in a random m-uple, which is equal to $\frac{m(m-1)}{(n-1)(n-2)}$, the infection probability λ, and the usual indicator function, yielding $\sum_{\ell \in \mathcal{V}\setminus\{i,j\}} \lambda \frac{m(m-1)}{(n-1)(n-2)} a_\ell x_j$.

Since all these events are independent and their occurrences are regulated by Poisson processes, the total rate at which j transmits the disease to i is computed by summing these three contributions [28], obtaining

$$\begin{aligned}\alpha_{ij}(\boldsymbol{x}) = \; & \lambda a_i \frac{m}{n-1} x_j + \lambda \frac{m}{n-1} a_j x_j \\ & + \lambda \frac{m(m-1)}{(n-1)(n-2)} x_j \sum\nolimits_{\ell \in \mathcal{V}\setminus\{i,j\}} a_\ell,\end{aligned} \tag{3}$$

whose summation over all $j \in \mathcal{V}$, ultimately yields (2a).

Finally, (2b) is obtained by observing that recovery for individual i is spontaneously triggered by a Poisson process with rate μ, independent of all the others. □

B. Derivation of the mean-field equations

Despite we are able to write the transition rates of the Markov process $\mathbf{x}(t)$ in Proposition 1, its analysis is hindered by the dimension of the state space $\{0,1\}^n$, which grows exponentially in the network size, and by the complexity of the transition rates. Hence, we follow the methodology proposed in [26] —already successfully applied to continuous-time ADNs [22], [23]— and we derive a continuous-state deterministic mean-field relaxation of the system's dynamics. The key idea is that, instead of tracking the evolution of the health state of each individual, we track the probability for each individual to be infected, i.e., the mean dynamics:

$$y_i(t) := \mathbb{P}[x_i(t) = 1] = \mathbb{E}[x_i(t)]. \tag{4}$$

Following [26], the dynamics of the variable vector $\mathbf{y}(t) = [y_1(t), \dots y_n(t)]$ from (4) is derived by approximating the expected value of the transition rates with the transition rates for the mean dynamics, i.e., approximating $\mathbb{E}[q_i^{01}(\mathbf{x}(t))] \approx q_i^{01}(\mathbb{E}[\mathbf{x}(t)]) = q_i^{01}(\mathbf{y}(t))$. Following this approach, the mean dynamics is approximated by a system of n ODEs.

Proposition 2. *The mean-field relaxation of the SIS model on an hADN is given by the solution of the following system of ODEs, with $i \in \mathcal{V}$,*

$$\begin{aligned}\dot{y}_i = (1-y_i)\lambda m \Big[& a_i \frac{1}{n-1} \sum_{j\in\mathcal{V}} y_j + \frac{1}{n-1} \sum_{j\in\mathcal{V}} a_j y_j \\ & + \frac{m-1}{(n-1)(n-2)} \sum_{j\in\mathcal{V}} y_j \sum_{\ell\in\mathcal{V}\setminus\{i,j\}} a_\ell \Big] - \mu y_i.\end{aligned} \tag{5}$$

Proof. According to (4), and using (1) and the mean-field approximation $\mathbb{E}[q_i^{01}(\mathbf{x})] \approx q_i^{01}(\mathbf{y}(t))$, we compute $\dot{y}_i(t) = \lim_{\Delta t \searrow 0} \frac{\mathbb{P}[x_i(t+\Delta t)=1] - \mathbb{P}[x_i(t)=1]}{\Delta t} = (1 - y_i(t)) q_i^{01}(\mathbf{y}) - y_i(t) q_i^{10}(\mathbf{y})$, from which (5) is obtained by inserting (2). □

Before presenting our main results, we define the first and second moment of the activity distribution as $\alpha_1 := \frac{1}{n}\sum_{i\in\mathcal{V}} a_i$ and $\alpha_2 := \frac{1}{n}\sum_{i\in\mathcal{V}} a_i^2$. Using α_2, we define the coefficient of variation as $c_v := \frac{\sqrt{\alpha_2}}{\alpha_1}$, which has minimal value $c_v = 1$ when the population is homogeneous ($a_i = \alpha_1$ for all $i \in \mathcal{V}$), and increases with the heterogeneity. Similarly, we define a macroscopic variable representing the average probability for a generic node to be infected as

$$z_1(t) := \frac{1}{n} \sum\nolimits_{i\in\mathcal{V}} y_i(t). \tag{6}$$

For $n \to \infty$, the epidemic prevalence for the stochastic model $I(t) := \frac{1}{n}|\{i \in \mathcal{V} : x_i(t) = 1\}|$ can be approximated for any finite time-horizon within an arbitrary precision [26] as $I(t) \approx z_1$. Hence, for sufficiently large networks, we can study the behavior of the epidemics at the population level by means of the mean-field equations in (5).

IV. Results

We start the analysis of the mean-field dynamics by establishing two preliminary results. First, we prove that the ODEs derived in Proposition 2 are well defined. Second, we prove that its trajectories always converge to an equilibrium.

Lemma 1. *$\mathcal{D} = [0,1]^n$ is positive invariant under* (5)*.*

Proof. $\mathcal{D}$ is compact and convex and (5) is Lipschitz-continuous; at $y_i = 0$, $\dot{y}_i \geq 0$ and at $y_i = 1$, $\dot{y}_i = -\mu < 0$. Hence, Nagumo's Theorem yields the claim [29]. □

Lemma 2. *The dynamics in* (5) *converges to an equilibrium.*

Proof. The Jacobian of (5) is Metzler, since its generic off-diagonal entry $J_{ij} = (1-y_i)\frac{\lambda m}{n-1}(a_i + a_j + \frac{m-1}{n-2}\sum_{\ell\neq i,j} a_\ell) \geq 0$. Hence, (5) is a monotone dynamical system [30] over the compact invariant domain $\mathcal{D}$ (Lemma 1). Therefore, all its trajectories converge to an equilibrium [30]. □

Lemma 2 guarantees that (5) always converges to an equilibrium. By observing (5), we can further make the following observation that characterizes possible equilibria.

Proposition 3. *The state $\hat{\mathbf{y}} = \mathbf{0}$ is always an equilibrium of* (5)*. Moreover, any other equilibrium, if present, has necessarily $\hat{y}_i > 0$ for all $i \in \mathcal{V}$.*

Proof. To show that $\hat{\mathbf{y}} = \mathbf{0}$ is an equilibrium is straightforward. The second claim is proved by contradiction. Assume that there exists an equilibrium $\hat{\mathbf{y}}$ with $\hat{y}_i = 0$ and $\hat{y}_j > 0$ for some $i \neq j \in \mathcal{V}$. Then, from (5), we get $\dot{y}_i \geq \frac{1}{n-1}\lambda m (a_i + a_j + \frac{m-1}{n-2}\sum_{\ell\neq i,j} a_\ell)\hat{y}_j > 0$, which contradicts the hypothesis that $\hat{\mathbf{y}}$ is an equilibrium. □

Based on Proposition 3, we can classify the equilibria of (5) into two main classes.

Definition 1. *Given an equilibrium $\hat{\mathbf{y}} \in [0,1]^n$ of* (5)*, we say that it is the disease-free equilibrium (DFE) iff $\hat{y}_i = 0$, $\forall i \in \mathcal{V}$, and an endemic equilibrium (EE) iff $\hat{y}_i > 0$, $\forall i \in \mathcal{V}$.*

Proposition 3 guarantees that the system has always a DFE. Moreover, other equilibria (viz., one or multiple EEs)

can be present. In the following, we focus our analysis on studying the epidemic threshold of the SIS model, i.e., the analytical condition under which the dynamical system undergoes a transition between a regime in which the DFE is globally asymptotically stable to a regime in which the DFE is unstable and trajectories converge to an EE, where each individual has a strictly positive probability of being infected. Such condition is derived in the following for large-scale networks, i.e., when $I(t) \approx z_1(t)$.

Theorem 1. *In the thermodynamic limit of $n \to \infty$, the epidemic threshold for* (5) *is*

$$\sigma = \frac{2}{m[(m+1)\alpha_1 + \sqrt{(m-1)(m+3)\alpha_1^2 + 4\alpha_2}]}. \quad (7)$$

If $\frac{\lambda}{\mu} < \sigma$, then the DFE is the unique globally asymptotically stable equilibrium of the system and all trajectories converges to it. If $\frac{\lambda}{\mu} > \sigma$, then the DFE is unstable and all trajectories with initial conditions different from the DFE converge to an EE.

Proof. To study the stability of the DFE, we observe that there is a one-to-one mapping between the DFE and the state $z_1 = 0$, i.e., $z_1 = 0 \iff \mathbf{y} = 0$. Hence, we can study the local stability of the DFE by studying the local stability of $z_1 = 0$. We follow a technique similar to the one used in [23] by defining the auxiliary variable

$$z_2 = \frac{1}{n}\sum\nolimits_{i\in\mathcal{V}} a_i y_i, \quad (8)$$

and considering the planar system (z_1, z_2). To derive such system, we use the fact that, in the limit of large networks,

$$\lim_{n\to\infty} \frac{1}{n-1}\sum_{i\in\mathcal{V}} y_i = \lim_{n\to\infty} \frac{1}{n}\sum_{i\in\mathcal{V}} y_i = z_1 \quad (9a)$$

$$\lim_{n\to\infty} \frac{1}{n-1}\sum_{i\in\mathcal{V}} a_i y_i = \lim_{n\to\infty} \frac{1}{n}\sum_{i\in\mathcal{V}} a_i y_i = z_2, \quad (9b)$$

$$\lim_{n\to\infty} \frac{1}{n-2}\sum_{\ell\in\mathcal{V}\setminus\{i,j\}} a_\ell = \lim_{n\to\infty} \frac{1}{n}\sum_{\ell\in\mathcal{V}} a_\ell = \alpha_1, \quad (9c)$$

for any $i, j \in \mathcal{V}$. Using (9), we write (5) as

$$\dot{y}_i = (1-y_i)\lambda m\big[a_i z_1 + z_2 + (m-1)\alpha_1 z_1\big] - \mu y_i, \quad (10)$$

and we compute

$$\dot{z}_1 = \frac{1}{n}\sum_{i\in\mathcal{V}} \dot{y}_i = -\mu z_1 + \lambda m\Big[\alpha_1 z_1 - z_1 z_2 + z_2(1-z_1) + (m-1)\alpha_1 z_1(1-z_1)\Big], \quad (11a)$$

$$\dot{z}_2 = \frac{1}{n}\sum_{i\in\mathcal{V}} a_i\dot{y}_i = -\mu z_2 + \lambda m\Big[\alpha_2 z_1 - z_1\frac{1}{n}\sum_{i\in\mathcal{V}} a_i^2 y_i + z_2(\alpha_1 - z_2) + (m-1)\alpha_1 z_1(\alpha_1 - z_2)\Big]. \quad (11b)$$

Finally, by linearizing these two equations about the origin, we obtain the following autonomous system:

$$\begin{aligned}\dot{z}_1 &= -\mu z_1 + \lambda m^2\alpha_1 z_1 + \lambda m z_2\\ \dot{z}_2 &= -\mu z_2 + \lambda m((m-1)\alpha_1^2 + \alpha_2) z_1 + \lambda m\alpha_1 z_2.\end{aligned} \quad (12)$$

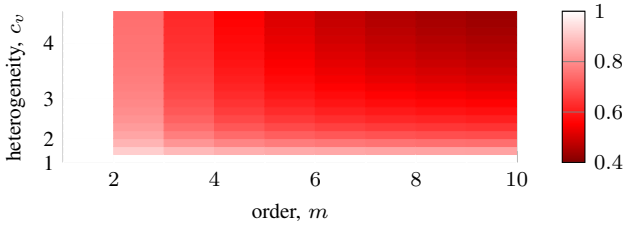

Fig. 2: Ratio between the threshold of an hADN and the one of an equivalent ADN from (14), for different values of m and c_v, with $\alpha_1 = 0.5$ and $\rho = 1$.

Then, we study local stability of the origin for (12), which is determined by the largest eigenvalue of its Jacobian matrix

$$J_{0,0} = \begin{bmatrix} \lambda m^2\alpha_1 - \mu & \lambda m \\ \lambda m((m-1)\alpha_1^2 + \alpha_2) & \lambda m\alpha_1 - \mu \end{bmatrix}, \quad (13)$$

yielding the condition in (7). Finally, we observe that the nonlinear terms in (10) are nonpositive. This, combined with the monotonicity of the system (Lemma 2) guarantees that a trajectory of the linearized system (which converge to the DFE) acts as upper-bound for the one of the nonlinear system, which then converges to the DFE. □

Remark 1. *For $m = 1$,* (7) *reduces to $\sigma = (\alpha_1 + \sqrt{\alpha_2})^{-1}$, as for the standard SIS model on ADNs [21], [22].*

The computation of the epidemic threshold in (7) allows us to to elucidate the nontrivial impact of higher-order interactions on the epidemic spreading by comparing (7) to the threshold for standard SIS model on ADNs, i.e., $\tilde{\sigma} = (M(\alpha_1 + \sqrt{\alpha_2}))^{-1}$, where M is the number of contacts established by an active individual. It is worth noticing that, each simplicial complex of order m generates exactly $m(m+1)/2$ pairwise contacts. Hence, to fairly compare standard networks and higher-order networks, we should consider a (standard) ADN with $M = m(m+1)/2$. By comparing the two thresholds, we obtain the ratio

$$\frac{\sigma}{\tilde{\sigma}} = \frac{\alpha_1 + \sqrt{\frac{(m^2+2m-3)\alpha_1^2 + 4\alpha_2}{m^2+2m+1}}}{\alpha_1 + \sqrt{\alpha_2}} = \frac{1 + \sqrt{1 + 4\frac{c_v^2 - 1}{(m+1)^2}}}{1 + c_v}. \quad (14)$$

From (14), we observe that the numerator cannot be larger than the denominator, being $c_v \geq 1$, with equality attained when $m = 1$ or $c_v = 1$. Therefore, we conclude that, for heterogeneous higher-order networks, the epidemic threshold is always strictly lower than the one on an ADN with the same average number of contacts. Figure 2 supports these analytical findings, illustrating how the higher-order nature of the network seems to favor the spread of epidemic diseases. In other words, if people are allowed to meet in larger groups, it becomes more difficult to keep an epidemic outbreak under control, since the DFE becomes unstable for lower values of the infection probability λ. This effect becomes more pronounced as the order of the network and the heterogeneity of the population increases.

A possible reason for this phenomenon lies in the fact that hADNs may exacerbate a phenomenon already seen in heterogeneous networks, whereby individuals who are more socially active are more likely to become infected and act as

superspreaders. In higher-order networks, such individuals not only are more likely to interact with others, but also to gather with multiple people, thereby giving rise to those superspreading events that are often indicated as key drivers of an epidemic outbreak [11].

V. SIS on hADNs with Behavioral Response

A. SIS model on adaptive hADNs

To capture the behavioral response to the epidemic spreading, we assume that infected individuals reduce their tendency to initiate social interactions, by temporarily reducing their activity. To capture this phenomenon, we introduce a parameter $\rho \in [0,1]$, inspired by [23], [31], and we define an adaptive version of the hADN defined in Section II-A by changing the rate of the Poisson clocks associated with each node i to the state-dependent value

$$\hat{a}_i(x_i(t)) := (1 - x_i(t)(1-\rho))a_i. \tag{15}$$

In other words, when susceptible ($x_i(t) = 0$), individual i has rate $\hat{a}_i = a_i$; when infected ($x_i(t) = 1$), the rate is reduced to $\hat{a}_i = \rho a_i$, where $\rho = 1$ means that infected individuals do not reduce their social activity, whereas the extreme case $\rho = 0$ captures the scenario in which infected nodes do not actively have social interactions. Note that, due to the memoryless property of Poisson processes, one can re-initialize the clock associated with an individual's activation each time the individual changes health state, without impacting the distribution of the stochastic process [27].

B. Dynamics

Similar to the standard SIS model on hADNs, also here all processes involved are independent Poisson processes, yielding a Markov chain, whose rates can be computed, similar to Proposition 1, as follows.

Proposition 4. *Consider an SIS model on a continuous-time hADN with behavioral response, the transition rates for a generic individual $i \in \mathcal{V}$ when $\mathbf{x}(t) = \mathbf{x}$ are equal to*

$$\begin{aligned} q_i^{01}(\mathbf{x}) &= \lambda a_i \frac{m}{n-1} \sum_{j\in\mathcal{V}} x_j + \lambda\rho \frac{m}{n-1} \sum_{j\in\mathcal{V}} a_j x_j \\ &+\lambda \frac{m(m-1)}{(n-1)(n-2)} \sum_{j\in\mathcal{V}} x_j \sum_{\ell\in\mathcal{V}\setminus\{i,j\}} a_\ell \\ &-\lambda(1-\rho) \frac{m(m-1)}{(n-1)(n-2)} \sum_{j\in\mathcal{V}} x_j \sum_{\ell\in\mathcal{V}\setminus\{i,j\}} a_\ell x_\ell, \end{aligned} \tag{16}$$

and $q_i^{10}(\mathbf{x}) = \mu$.

Proof. The proof follows the same arguments used for Proposition 1. The main difference is that the activity rate of a generic individual $\ell \in \mathcal{V}$ is now state-dependent and equal to $\hat{a}_\ell(x_\ell) = a_\ell(1 - x_\ell(1-\rho))$. This should be considered when deriving the three contributions to $\alpha_{ij}(\boldsymbol{x})$: in the first contribution, the node who initiates the interaction is i, who is susceptible ($\hat{a}_i(x_i) = a_i$). In the second term, the interaction is initiated by j, who is infected ($\hat{a}_j(x_j) = \rho a_j$). Finally, in the third term, we have no information on the health state of ℓ, so we need to use its general expression, which can be re-written as $\hat{a}_\ell(x_\ell) = a_\ell - (1-\rho)a_\ell x_\ell$, thereby splitting the last contribution into two distinct terms, one always positive and one always negative (and not larger than the first one) obtaining

$$\begin{aligned} \alpha_{ij}(\mathbf{x}) &= \lambda a_i \frac{m}{n-1} x_j + \lambda\rho \frac{m}{n-1} a_j x_j \\ &+\lambda \frac{m(m-1)}{(n-1)(n-2)} x_j \sum\nolimits_{\ell\in\mathcal{V}\setminus\{i,j\}} a_\ell \\ &-\lambda(1-\rho) \frac{m(m-1)}{(n-1)(n-2)} x_j \sum\nolimits_{\ell\in\mathcal{V}\setminus\{i,j\}} a_\ell x_\ell. \end{aligned} \tag{17}$$

Finally, (19) is obtained by summing (17) over all $j \in \mathcal{V}$. □

Following the mean-field approach described in Section III-B, the mean dynamics $y_i(t)$ in the presence of behavioral response is approximated by the following system of ODEs, whose derivation follows the same procedure of Proposition 2 using (16) instead of (2a), and is omitted.

Proposition 5. *The mean-field relaxation of the SIS model with behavioral response on hADN is given by the solution of the following system of ODEs, for $i \in \mathcal{V}$:*

$$\begin{aligned} \dot{y}_i &= (1-y_i)\lambda m \Big[\frac{a_i}{n-1} \sum_{j\in\mathcal{V}} y_j + \frac{\rho}{n-1} \sum_{j\in\mathcal{V}} a_j y_j \\ &+\frac{m-1}{(n-1)(n-2)} \sum_{j\in\mathcal{V}} y_j \sum_{\ell\in\mathcal{V}\setminus\{i,j\}} a_\ell \\ &-\frac{(1-\rho)(m-1)}{(n-1)(n-2)} \sum_{j\in\mathcal{V}} y_j \sum_{\ell\in\mathcal{V}\setminus\{i,j\}} a_\ell y_\ell \Big] - \mu y_i. \end{aligned} \tag{18}$$

C. Results

First, we observe that it is straightforward to prove that Lemmas 1 and 2 are still valid for (18), and thus the dynamics is well defined and all trajectories converge to an equilibrium. Moreover, the same classification of the equilibria into a DFE (always present) and one or multiple EEs in Definition 1 is possible by generalizing Proposition 3. Therefore, we study the behavior of the epidemics on hADNs with behavioral response by establishing the following result, whose proof (which follows the same line of arguments used to prove Theorem 1) is omitted due to space constraints.

Theorem 2. *In the thermodynamic limit of $n \to \infty$, the epidemic threshold for* (18) *is*

$$\sigma := \frac{2}{m[(m+1)\alpha_1 + \sqrt{(m^2 + 2\rho m + \rho^2 - 4\rho)\alpha_1^2 + 4\alpha_2}]} \tag{19}$$

If $\frac{\lambda}{\mu} < \sigma$, then the DFE is the unique globally asymptotically stable equilibrium of the system and all trajectories converges to it. If $\frac{\lambda}{\mu} > \sigma$, then the DFE is unstable and all trajectories with initial conditions different from the DFE converge to an EE.

Remark 2. *When $m = 1$,* (19) *reduces to the one of an SIS model on standard ADNs with behavioral response [31].*

Using Theorem 2, we investigate the impact of the interactions (m), the behavioral response (ρ), and the population heterogeneity (c_v) on the epidemic spreading. First, we

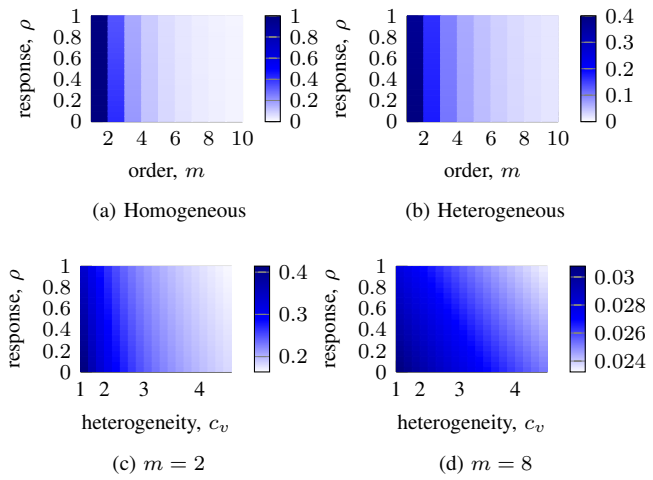

(a) Homogeneous (b) Heterogeneous

(c) $m = 2$ (d) $m = 8$

Fig. 3: Threshold in (7) evaluated for different values of the parameters. In (a-b), different m and ρ for (a) a homogeneous population with $\alpha_1 = 0.5$ ($c_v = 1$) and (b) a heterogeneous population with $\alpha_1 = 0.5$ and $\alpha_2 = 5$ ($c_v \approx 4.47$); in (c-d), different c_v and ρ for (c) $m = 2$ and (d) $m = 8$.

observe that the impact of the order m is dominant (Figs. 3a and 3b). This provides further support for banning large gatherings to contain epidemic outbreaks. Second, when m is fixed, the impact of the behavioral response and heterogeneity depend on the order of the network: for small m, heterogeneity has a key impact and the response is very marginal (Fig. 3c); as m increases, the impact of ρ becomes larger (Fig. 3d), highlighting the importance of testing before joining large events during an epidemic outbreak.

VI. Conclusion

We proposed and studied a novel continuous-time framework to model epidemics on complex networks, characterized by time-varying higher-order interactions. Extending the paradigm of ADNs and employing a mean-field approach, we gained analytical insights into how the presence of higher-order interactions —which capture superspreading events— shapes the epidemic outbreak. In particular, our results provided evidence that large gatherings can favor contagion, supporting their ban during epidemic outbreaks.

Our results pave the way for many lines of future research. First, further efforts should be placed into characterizing EEs. Second, Section V has shown how hADNs are amenable to extensions. We aim to consider more realistic decision-making processes (e.g., using game-theoretic models or opinion dynamics), as well as incorporate explicit control actions (e.g., lock-downs or vaccination campaigns). Third, the success of hADNs in obtaining an analytically-tractable framework to study epidemic spreading suggests that other phenomena driven by interactions that involve more than just two entities at a time can be studied using hADNs.

References

[1] C. Nowzari, V. M. Preciado, and G. J. Pappas, "Analysis and control of epidemics: a survey of spreading processes on complex networks," *IEEE Control Syst. Mag.*, vol. 36, no. 1, pp. 26–46, 2016.

[2] W. Mei, S. Mohagheghi, S. Zampieri, and F. Bullo, "On the dynamics of deterministic epidemic propagation over networks," *Annu. Rev. Contr.*, vol. 44, pp. 116–128, 2017.

[3] P. E. Paré, C. L. Beck, and T. Başar, "Modeling, estimation, and analysis of epidemics over networks: An overview," *Annu. Rev. Control*, vol. 50, pp. 345–360, 2020.

[4] L. Zino and M. Cao, "Analysis, prediction, and control of epidemics: A survey from scalar to dynamic network models," *IEEE Circuits Syst. Mag.*, vol. 21, no. 4, pp. 4–23, 2021.

[5] G. Giordano *et al.*, "Modelling the COVID-19 epidemic and implementation of population-wide interventions in Italy," *Nat. Med.*, vol. 26, pp. 855–860, 2020.

[6] F. Della Rossa *et al.*, "A network model of Italy shows that intermittent regional strategies can alleviate the COVID-19 epidemic," *Nat. Comm.*, vol. 11, no. 1, p. 5106, 2020.

[7] R. Carli, G. Cavone, N. Epicoco, P. Scarabaggio, and M. Dotoli, "Model predictive control to mitigate the COVID-19 outbreak in a multi-region scenario," *Annu. Rev. Control*, vol. 50, pp. 373–393, 2020.

[8] G. C. Calafiore, C. Novara, and C. Possieri, "A time-varying SIRD model for the COVID-19 contagion in Italy," *Annu. Rev. Control*, vol. 50, pp. 361–372, 2020.

[9] F. Parino, L. Zino, M. Porfiri, and A. Rizzo, "Modelling and predicting the effect of social distancing and travel restrictions on COVID-19 spreading," *J. R. Soc. Interface*, vol. 18, no. 175, p. 20200875, 2021.

[10] M. Ogura, V. M. Preciado, and N. Masuda, "Optimal containment of epidemics over temporal activity-driven networks," *SIAM J. Appl. Math.*, vol. 79, no. 3, pp. 986–1006, 2019.

[11] J. E. Lemieux *et al.*, "Phylogenetic analysis of SARS-CoV-2 in Boston highlights the impact of superspreading events," *Science*, vol. 371, no. 6529, 2021.

[12] C. Bick, E. Gross, H. A. Harrington, and M. T. Schaub, "What are higher-order networks?" *SIAM Rev.*, vol. 65, no. 3, pp. 686–731, 2023.

[13] G. Bianconi, *Higher-Order Networks*, 2021.

[14] S. Boccaletti *et al.*, "The structure and dynamics of networks with higher order interactions," *Phys. Rep.*, vol. 1018, pp. 1–64, 2023.

[15] W. Wang, Y. Nie, W. Li, T. Lin, M.-S. Shang, S. Su, Y. Tang, Y.-C. Zhang, and G.-Q. Sun, "Epidemic spreading on higher-order networks," *Phys. Rep.*, vol. 1056, p. 1–70, 2024.

[16] P. Cisneros-Velarde and F. Bullo, "Multigroup SIS epidemics with simplicial and higher order interactions," *IEEE Trans. Control Netw. Syst.*, vol. 9, no. 2, pp. 695–705, 2022.

[17] J. Fan, Q. Yin, C. Xia, and M. Perc, "Epidemics on multilayer simplicial complexes," *Proc. R. Soc. A*, vol. 478, no. 2261, 2022.

[18] G. Petri and A. Barrat, "Simplicial activity driven model," *Phys. Rev. Lett.*, vol. 121, p. 228301, 2018.

[19] S. Huang, Y.-H. Xu, M.-Y. Li, and M.-B. Hu, "Effect of behavioral changes on epidemic spreading in coupled simplicial activity driven networks," *J. Stat. Mech*, vol. 2023, no. 12, p. 123405, 2023.

[20] S. Zhang, D. Zhao, C. Xia, and J. Tanimoto, "Impact of simplicial complexes on epidemic spreading in partially mapping activity-driven multiplex networks," *Chaos*, vol. 33, no. 6, 2023.

[21] N. Perra, B. Gonçalves, R. Pastor-Satorras, and A. Vespignani, "Activity driven modeling of time varying networks," *Sci. Rep.*, vol. 2, 2012.

[22] L. Zino, A. Rizzo, and M. Porfiri, "Continuous-time discrete-distribution theory for activity-driven networks," *Phys. Rev. Lett.*, vol. 117, 2016.

[23] ——, "On assessing control actions for epidemic models on temporal networks," *IEEE Control Syst. Lett.*, vol. 4, no. 4, pp. 797–802, 2020.

[24] K. Frieswijk, L. Zino, M. Ye, A. Rizzo, and M. Cao, "A mean-field analysis of a network behavioral–epidemic model," *IEEE Control Syst. Lett.*, vol. 6, pp. 2533–2538, 2022.

[25] A. R. Hota, T. Sneh, and K. Gupta, "Impacts of game-theoretic activation on epidemic spread over dynamical networks," *SIAM J. Control Optim.*, vol. 60, no. 2, pp. S92–S118, 2022.

[26] P. V. Mieghem, J. Omic, and R. Kooij, "Virus spread in networks," *IEEE/ACM Trans. Netw.*, vol. 17, no. 1, pp. 1–14, Feb 2009.

[27] D. A. Levin, Y. Peres, and E. L. Wilmer, *Markov chains and mixing times*. Providence RI, US: American Mathematical Society, 2006.

[28] N. T. J. Bailey, *The Elements of Stochastic Processes with Applications to the Natural Sciences*, 1990.

[29] F. Blanchini, "Set invariance in control," *Automatica*, vol. 35, no. 11, pp. 1747–1767, 1999.

[30] H. L. Smith, *Monotone Dynamical Systems: An Introduction to the Theory of Competitive and Cooperative Systems*, 2008, no. 41.

[31] A. Rizzo, M. Frasca, and M. Porfiri, "Effect of individual behavior on epidemic spreading in activity driven networks," *Phys. Rev. E*, vol. 90, 2014.